IEEE Photonics Journal
An IEEE Photonics Society Publication

Open Access

# Performance Evaluation of High-Speed Polar Coded CO-OFDM System with Nonlinear and Linear Impairments

Volume 9, Number 4, August 2017

Ling Liu
Shilin Xiao
Meihua Bi
Jiafei Fang
Yunhao Zhang
Weisheng Hu

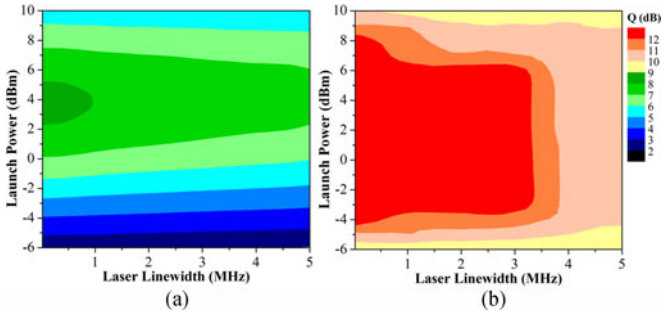


DOI: 10.1109/JPHOT.2017.2711278
1943-0655 

# Performance Evaluation of High-Speed Polar Coded CO-OFDM System with Nonlinear and Linear Impairments

**Ling Liu,[1] Shilin Xiao,[1] Meihua Bi,[1,2] Jiafei Fang,[1] Yunhao Zhang,[1] and Weisheng Hu[1]**

[1]State Key Lab of Advanced Optical Communication Systems and Networks, Shanghai Jiao Tong University, Shanghai 200240, China
[2]College of Communication Engineering, Hangzhou Dianzi University, Hangzhou 310018, China

*DOI:10.1109/JPHOT.2017.2711278*


Manuscript received April 22, 2017; revised May 27, 2017; accepted May 31, 2017. Date of publication June 5, 2017; date of current version June 20, 2017. (Corresponding author: Shilin Xiao (e-mail: slxiao@sjtu.edu.cn).

**Abstract:** In this paper, the performance of polar code in high-speed coherent optical orthogonal frequency division multiplexing (CO-OFDM) system with nonlinear and linear impairments is comprehensively investigated for the first time. Results show that soft decision-based polar code is slightly affected by nonlinearity-induced non-Gaussian noise but still performs strong robustness. In the nonlinear domain of single-channel 40-Gb/s CO-OFDM at 320-km of transmission, with the help of polar code, the nonlinear tolerance is extended by 4 dB and a maximum code gain (in Q-factor) of 5.9 dB is achieved under symmetric dispersion compensation. Meanwhile, polar code significantly resists linear impairment in both nonlinear and linear domains.

**Index Terms:** Coherent optical orthogonal frequency division multiplexing (CO-OFDM), polar code, nonlinear impairment, linear impairment.

## 1. Introduction

To adapt to the ever-increasing demand of transmission capacity and data rate in the fiber-optic community [1], coherent optical orthogonal frequency division multiplexing (CO-OFDM) has attracted a lot of interest due to its high spectral efficiency, dispersion resilience, superior receiver sensitivity and low-complexity digital signal processing (DSP) [2]–[4]. However, there are two categories of impairments in high-speed CO-OFDM system, linear and nonlinear impairments. The linear impairment mainly contains dispersion, and the nonlinear impairment mainly contains fiber nonlinearity and laser phase noise [5], [6]. Firstly, fiber nonlinearity will impose restrictions on the maximum achievable data rate as well as transmission distance and cause severe signal degradation [7], [8], due to the fact that the high peak-to-average power ratio (PAPR) of OFDM makes it vulnerable to nonlinear effects [9]. Secondly, laser phase noise will introduce inter-carrier interference (ICI) [10] which causes the loss of orthogonality among OFDM subcarriers [11] and is difficult to mitigate, as a result, the system performance is severely degraded. Forward error correction (FEC), as an effective method to improve overall system performance, has been extensively used in optical communication systems to guarantee quasi error-free transmission despite transmission impairments [12], in particular, next generation optical transmission systems tend to

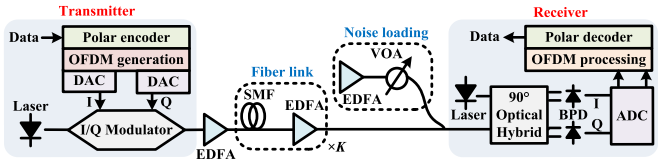


Fig. 1. Configuration of single-channel polar coded CO-OFDM system. DAC: digital to analog convertor, I/Q modulator: in-phase/quadrature modulator, EDFA: erbium doped fiber amplifier, SMF: single mode fiber, VOA: variable optical attenuation, BPD: balanced photo diode, ADC: analog to digital convertor.

employ soft decision-based FEC solutions rather than hard decision case due to their superior performance [13].

In our previous work [14], the polar code, as a novel soft decision-based and provable Shannon capacity-achieving code with low complexity [15], [16], was introduced and experimentally demonstrated in CO-OFDM system for the first time to achieve high-performance cost-effective long-haul transmission. However, in the nonlinear domain of CO-OFDM system where nonlinearity-induced non-Gaussian noise exists, it is unclear whether the soft decision-based polar code necessarily yields optimal performance since the channel assumption of additive white Gaussian noise (AWGN) used for soft decision is not valid [17], [18].

To further study the polar code in high-speed CO-OFDM system, for the first time, this paper comprehensively investigates the behavior of polar code under nonlinear and linear impairments. It is well known that for the high-speed transmission operating at 40 Gb/s and above, the major nonlinear penalties are from intra-channel nonlinearities rather than inter-channel nonlinearities [19]. Thus the performance of single-channel 40-Gb/s polar-coded CO-OFDM system is evaluated with higher order modulation format and inadequate DSP under three different dispersion maps, since the dispersion compensation plays an important role in the nonlinear mitigation [10]. Results show that the performance of polar code is slightly affected by nonlinear impairments but still performs strong robustness. Aided by polar code, in nonlinear domain of single-channel 40-Gb/s CO-OFDM at 320-km of transmission, the optimal fiber launch power is increased by 4 dB and a maximum code gain (in Q-factor) of 5.9 dB is achieved under symmetric dispersion compensation. The remainder of this paper is organized as follows. Section 2 describes the system setup and parameter setting, also, theoretically analyzes the effect of nonlinearities on polar code. Section 3 first presents the simulation results of the performance of polar coding under nonlinear and linear impairments in three dispersion map schemes, and then verifies them by experiment. Conclusions are given in Section 4.

## 2. System Setup and Theoretical Analysis

Following the system configuration in Fig. 1 and generation/post-processing procedures of polar coded CO-OFDM signal detailed in our previous work [14], Monte-Carlo simulation is conducted using commercial software OptiSystem 7.0 and MATLAB. The electrical parts, including the polar encoder, OFDM generation, OFDM processing and polar decoder, are implemented in MATLAB. All the optical parts are implemented in OptiSystem 7.0. At the transmitter, the original data $U$ is first encoded by polar code of length $N = 512$, code rate $R = 0.5$ and code unit $d = 800$ ($d = u/N/R$, $u$ is the length of $U$). The polar coded data in each code unit $x_p$ ($p = 1, 2, 3, \ldots, N$) is denoted by

$$x = U \cdot G_N = U \cdot B_N \cdot \begin{bmatrix} 1 & 0 \\ 1 & 1 \end{bmatrix}^{\otimes n} \tag{1}$$

where $G_N$ is the generator matrix, $B_N$ is the bit-reversal operation and $\otimes n$ denotes the $n$th ($n = log_2 N$) Kronecker power of the matrix [15]. Then M-quadrature amplitude modulation (QAM) OFDM modulation is adopted. To obtain the signal transmission rate $R_{OFDM}$ of 40 Gb/s, for the total number of subcarriers $N_{sc}$, $N_{sc}/2$ subcarriers are set as data subcarriers $N_{data}$ [9] mapped with 16-QAM polar coded data $X_q$ ($q = 1,2, .., N \cdot d/m$, $m = log_2 M$, $M = 16$), while zeros occupy the remaining

subcarriers to act as guard band and spectrally separate the baseband from high frequency aliasing products [20]. The cyclic prefix (CP) length is 1/8 of the fast Fourier transform (FFT) size $N_{FFT}$. The total number of measured symbols is $N_s = N \cdot d/(m \cdot N_{data})$. The polar coded OFDM symbol can be expressed as

$$S_B(t) = \sum_{k=1}^{N_{sc}} e^{j2\pi f_k t} C_k \tag{2}$$

where $f_k$ is the frequency of *k-th* subcarrier, $C_k$ is the *k-th* polar coded OFDM data. The in-phase (I) and quadrature (Q) components of the generated polar coded OFDM signal $S_B(t)$ are sampled by two digital-to-analog convertors (DACs) with sampling rate $S$ of 20 GS/s and then are used to drive the I/Q modulator biased at the null point to get linear electrical/optical conversion, the corresponding data rate is 40 Gb/s ($R_{OFDM} = S \cdot log_2(M) \cdot N_{data}/N_{sc}$). The laser centered at wavelength $\lambda_0$ of 1550 nm serves as optical source. An erbium doped fiber amplifier (EDFA) is deployed after the I/Q modulator to boost the optical polar coded CO-OFDM signal $S(t) = e^{j\omega t+\phi} \cdot S_B(t)$, where $\omega$ and $\phi$ are the frequency and phase of the laser respectively. The fiber link consists of $K = 4$ spans of 80-km standard single mode fiber (SMF) and an EDFA of 16-dB gain and 6-dB noise figure. The SMF has the loss $\alpha$ of 0.2 dB/km, dispersion parameter $D$ of 16.75 ps/nm/km, dispersion slope of 0.075 ps/nm$^2$/km, differential group delay $\beta_1$ of 0.2 ps/km, second-order group velocity dispersion $\beta_2$ ($\beta_2 = -\lambda_0^2 D/(2\pi c)$, where $c$ is the speed of light in vacuum) of $-21.35$ ps$^2$/km, the nonlinear refractive index coefficient $n_2$ of $2.6 \times 10^{-20}$ m$^2$/W and fiber effective area $A_{\text{eff}}$ of 80 $\mu$m$^2$. The corresponding nonlinear Schröinger equation [21] for $S(t)$ can be simplified as

$$\frac{\partial S}{\partial z} + \frac{\alpha}{2} S + \beta_1 \frac{\partial S}{\partial t} + j\frac{\beta_2}{2}\frac{\partial^2 S}{\partial t^2} = j\frac{2\pi n_2}{\lambda_0 A_{eff}}|S|^2 S \tag{3}$$

At the receiver, the received optical signal beats with the local laser signal in a 90° optical hybrid whose four outputs are injected into a pair of balanced photo diodes (BPDs) to obtain the I and Q components of the received polar coded CO-OFDM signal. After sampled by analog to digital convertors (ADCs), OFDM post-processing is performed first. Assume that the signal before 16-QAM demodulation is labeled as $y_p = y_{p,Re} + i \cdot y_{p,Im}$, $x_k^{q,0}$ denotes the demapping condition when $x_{mp-m+q} = 0\,(k = 1, 2, 3\ldots, 2^{m-1}$, $p = 1, 2, 3\ldots, N/m$, $q = 1, 2, 3\ldots, m)$, $x_k$ can be expressed as $x_k = x_{k,Re} + i \cdot x_{k,Im}$ since it's a complex number. Soft decision which presents a reliability measure of each bit being 1 or 0 for a certain symbol is based on the assumption of AWGN channel with zero mean and variance $\sigma^2$, the prior probability $P(y|x)$, i.e. channel transition probability, is given as

$$\begin{aligned} P\left(y_p | x_{mp-m+q} = b\right) &= \sum_{k=1}^{2^{m-1}} P\left(y_{p,\text{Re}}, x_{k,\text{Re}}^{q,b}\right) \cdot P\left(y_{p,\text{Im}}, x_{k,\text{Im}}^{q,b}\right) \\ &= \sum_{k=1}^{2^{m-1}} \frac{1}{\sigma\sqrt{2\pi}} \exp\left(-\frac{\left(y_{p,\text{Re}} - x_{k,\text{Re}}^{q,b}\right)^2}{\sigma^2}\right) \cdot \frac{1}{\sigma\sqrt{2\pi}} \exp\left(-\frac{\left(y_{p,\text{Im}} - x_{k,\text{Im}}^{q,b}\right)^2}{\sigma^2}\right) \end{aligned} \tag{4}$$

where $b = 0,1$. The corresponding posterior probability $P(x|y)$ is

$$P\left(x_{mp-m+q} = b | y_p\right) = \frac{P\left(y_p | x_{mp-m+q} = b\right)}{P\left(y_p | x_{mp-m+q} = 0\right) + P\left(y_p | x_{mp-m+q} = 1\right)} \tag{5}$$

Then, the consequent polar decoding finds the maximum posterior probability among $P(x|y)$ based on successive cancellation list (SCL) algorithm using a list size of 4 for bit recovering [14], [22]. Therefore, the channel model will affect the transition probability and soft decision, consequently, deviations can be expected in the behavior of polar code. In the nonlinear domain of CO-OFDM system where the nonlinearity-induced non-Gaussian noise exists [17], [18], the initial assumption

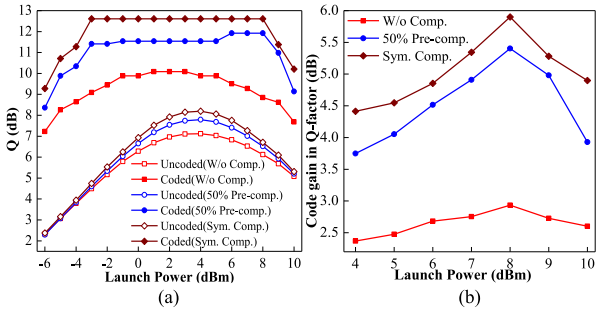


Fig. 2. (a) Q-factor as a function of fiber launch power for conventional and polar coded 40-Gb/s CO-OFDM signals and (b) polar code gain in Q-factor versus fiber launch power in three different dispersion map schemes after 320-km transmission under a combined laser linewidth of 20 kHz.

of channel model is not valid anymore, thus the accuracy of the polar decoding is decreased compared with the AWGN case.

## 3. Results and Analysis

### 3.1 Simulation Results

First, nonlinear impairment, which mainly includes fiber nonlinearity and laser phase noise, is discussed [6]. To only evaluate the tolerance of polar code to fiber nonlinearity, we first minimize the laser phase noise by reducing laser linewidth and FFT size [10]. Because laser phase noise $\phi(n')$ will lead to ICI [4] whose coefficient *I(k)* is denoted as

$$I(k) = \frac{1}{N_{FFT}} \sum_{n=0}^{N_{FFT}-1} \exp\left[ j\frac{2\pi kn}{N_{FFT}} + j\phi\left(n'\right) \right], \ \sigma_{\phi}^{2}(T) = 2\pi f_{3dB} T \tag{6}$$

where $T$ is the sampling period, $\sigma_{\phi}$ is standard deviation of $\phi(n')$ and $f_{3dB}$ is the 3-dB bandwidth of the Lorentzian shape of the laser [23], [24], indicating that ICI power can be reduced by decreasing $f_{3dB}$ and $N_{FFT}$. Thus, laser linewidths $f_{3dB}$ at the transmitter and receiver are both set to 10 kHz which is the same as the experimental laser, the FFT size $N_{FFT}$ is set to 128, similar to [10]. The corresponding number of data subcarriers is 64, CP length is 16 and the number of measured symbols is 1600. 16 training symbols are periodically inserted for channel estimation and phase noise compensation [25]. Owing to the fact that the nonlinear mitigation depends on dispersion compensation scheme [10], three different dispersion map schemes are investigated which are fiber links without dispersion compensation (W/o Comp.), with half pre-compensation (50% Pre-comp.) to obtain a symmetric dispersion map along the link [21], with half pre- and half post-compensation (known as symmetric compensation, abbreviated as Sym. Comp. [10]) respectively. The dispersion compensation is based on dispersion compensation fiber (DCF), which is the same as that used in the practical backbone network. DCF of $-2680$ ps/nm, which is half of the cumulative dispersion along the 320-km link, is applied before the first span to introduce half pre-compensation or after the last span to perform half post-compensation [21].

Fig. 2(a) demonstrates the Q-factor as a function of fiber launch power in three different dispersion map schemes for conventional and polar coded 40-Gb/s CO-OFDM signals after 320-km transmission. Note that Q-factor, as an assessment of system performance, is estimated from the bit error rate (BER) obtained by error counting after hard-decision for conventional (uncoded) signal or soft-decision for polar coded signal, measured by $\mathrm{Q} = 20\log_{10}[2^{1/2} erfc^{-1}(2BER)]$ [26]. Results show that when the launch power is higher than 4 dBm, signal undergoes nonlinear domain where nonlinear impairment dominates over linear impairment. The performance improvement brought by polar code is apparent when compared to the conventional case. It is interesting to observe that for conventional signal, the tolerable launch power offset for a fixed Q-factor in nonlinear domain

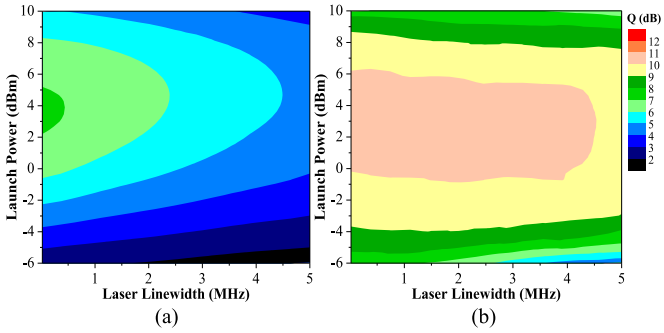


Fig. 3. Contour plots of Q-factor versus launch power and laser linewidth for (a) conventional and (b) polar coded 40-Gb/s CO-OFDM signals after dispersion-unmanaged 320-km transmission.

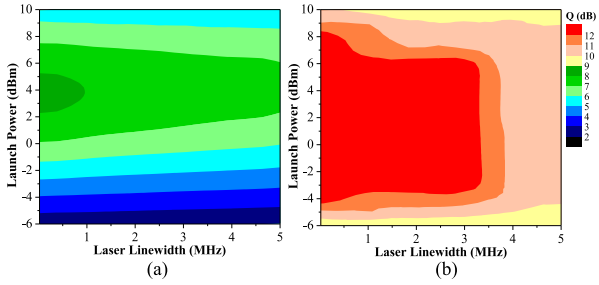


Fig. 4. Contour plot of Q-factor versus launch power and laser linewidth for (a) conventional and (b) polar coded 40-Gb/s CO-OFDM signals after symmetric dispersion-compensated 320-km transmission.

is symmetric with that in linear domain, while for polar coded signal, the tolerance in nonlinear domain is smaller than that in linear domain. The phenomena agree with the theoretical analysis in Section 2 that the non-Gaussian noise in nonlinear domain affects the performance of polar code. When dispersion compensation is applied, the Q-factor is improved. It is worth noting that the improvement is more pronounced for polar coded signal compared to the conventional case, the corresponding code gain (in Q-factor) in nonlinear domain as a function of launch power is depicted in Fig. 2(b). It is shown that polar code extends the optimum fiber launch power to 8 dBm from 4 dBm, that is, a 4-dB improvement in nonlinear tolerance is achieved in any dispersion map scheme. When the launch power is higher than 8 dBm, code gain decreases because higher order nonlinearities will significantly affect the AWGN channel model which results in the inaccuracy of polar decoding. For different dispersion map schemes, the maximum code gains (in Q-factor) of 3 dB, 5.4 dB and 5.9 dB are obtained in unmanaged, pre-compensation and symmetric compensation schemes respectively, clearly indicating the benefit of symmetric compensation scheme, especially for polar coded signal which further enhances the code gain by 2.9 dB. These phenomena attribute to the fact that symmetric compensation scheme enhances the similarity of distortions on neighboring OFDM subcarriers [2] which makes transition probability of each channel in polar decoding more consistent, and also, it mitigates the dispersion-induced inter-symbol interference which cyclic prefix and symbol duration of the OFDM signal are insufficiently long to combat for a long transmission link. The results above verify that polar code can still mitigate the non-Gaussian distributed noise-induced performance deterioration to some extent, which is suitable for the nonlinear region of CO-OFDM system.

Then, without loss of generality, the performance of polar code in 40-Gb/s CO-OFDM system with both fiber nonlinearity and laser phase noise is studied comprehensively. Fig. 3 demonstrates the contour plots of Q-factor versus launch power and combined laser linewidth after 320-km dispersion-unmanaged transmission. For a fixed launch power, as laser linewidth varies from 0 MHz to 5 MHz, the Q-factor of polar coded signal remains almost unchanged as depicted in

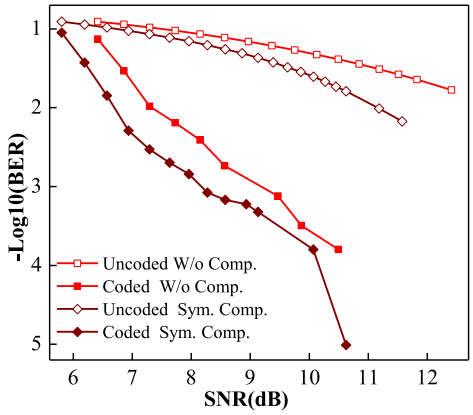


Fig. 5. BER versus electrical SNR for conventional and polar coded 40-Gb/s CO-OFDM signals after dispersion-unmanaged and symmetric dispersion-compensated 320-km transmissions when the optimal launch power is applied under a combined laser linewidth of 20 kHz.

Fig. 3(b), while the Q-factor of conventional signal decreases massively as shown in Fig. 3(a) which can be told from the gradient represented by color. It reveals that polar coded CO-OFDM system is insensitive to laser linewidth under any launch power, that is, the capability to resist linear impairment stays constant under any nonlinear impairment. For a fixed combined laser linewidth, as the launch power varies from $-6$ dBm to 10 dBm, compared to the conventional signal, polar coded signal has higher optimum launch power and larger power range that maintains the same Q-factor. It indicates the improved robustness against nonlinearity under any linear impairment aided by polar code. Similarly, for symmetric dispersion compensation scheme, Fig. 4 shows the contour plots of Q-factor versus launch power and combined laser linewidth. For a fixed launch power, the difference in laser linewidth tolerance between conventional signal in Fig. 4(a) and polar coded signal in Fig. 4(b) is smaller compared with Fig. 3. The reason is that symmetric dispersion compensation can partly neutralize performance degradation brought by linewidth. Similarly, for a fixed laser linewidth, the polar coded signal is less sensitive to launch power and has higher optimum power compared with conventional case. Hence, polar code has excellent tolerance to both nonlinear and linear impairment. When comparing Fig. 4(a) with Fig. 3(a), it can be known that under symmetric dispersion compensation, the Q-factor improves while the reachable optimum launch power stays almost the same, indicating that for conventional signal, symmetric dispersion compensation can partly improve the system performance in both linear and nonlinear regions but cannot strengthen the nonlinear tolerance. When comparing Fig. 4(b) with Fig. 3(b), it can be seen that for polar coded signal, Q-factor and nonlinear tolerance are both enhanced when symmetric dispersion compensation is applied. It can be concluded that nonlinear and linear impairments are both mitigated by polar code effectively, what is more, when symmetric dispersion compensation is adopted, they are further alleviated.

At last, the performance of polar code in mitigating linear impairment is also clearly demonstrated. By applying the optimal fiber launch power 4 dBm and setting laser linewidths at transmitter and receiver both low as 10 kHz, the nonlinear impairment is minimized. Fig. 5 depicts the BER versus electrical signal noise ratio (SNR) for the conventional and polar coded 40-Gb/s CO-OFDM signals after dispersion-unmanaged and symmetric dispersion-compensated 320-km transmissions. It shows that at BER of $2 \times 10^{-3}$, polar code gains (in SNR) of 4.5 dB and 6.2 dB are obtained under dispersion-unmanaged and symmetric dispersion-compensated schemes respectively.

### *3.2 Experiment verification*

The experiment is conducted to evaluate the performances of conventional and polar coded CO-OFDM signals in linear and nonlinear regions to verify the conclusions obtained from subsection

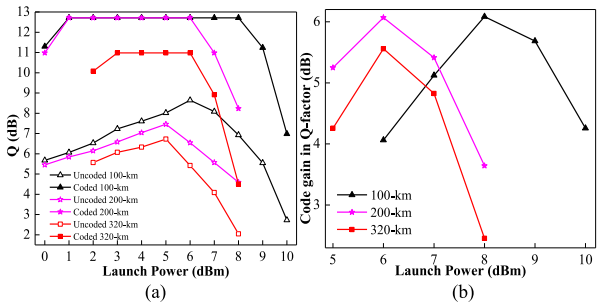


Fig. 6. Experimental results of (a) Q-factor for conventional and polar coded 25-Gb/s CO-OFDM signals and (b) the corresponding polar code gain in Q-factor versus fiber launch power over various transmission distances.

3.1. At the transmitter, the output of a continuous-wave laser (Koheras AdjustiK-E15) at 1550 nm passes through a polarization controller which is precisely adjusted before injecting into the I/Q modulator (FUJITSU FTM7960EX) to get the best modulation performance. I and Q components of the polar coded OFDM signal which are generated offline in MATLAB are loaded into the arbitrary wave generator (AWG, Tektronix AWG7122C) with 20-GS/s sampling rate. Two output channels are first amplified by two high-linearity electrical amplifiers (Analog Devices Inc. ADL5240) respectively to mitigate the inherent unsatisfactory frequency response of AWG [11], and then drive the I/Q modulator biased at the null point to achieve a linear RF-to-optical conversion and eliminate the modulator nonlinearity [3], [5]. The output optical polar coded OFDM signal from the I/Q modulator is first amplified by an EDFA (WXZTE-WZEDFA) and then transmits through the loop which consists of the SMF and EDFA. After fiber transmission, the output of an EDFA functions as noise loading to adjust the SNR, together with a variable optical attenuator (VOA). At the receiver, the received signal passes through a polarization controller first and then injects into a 90° optical hybrid (Kylia COH28-X), together with the output of local oscillator (Koheras AdjustiK-E15). Four outputs of the hybrid are detected by a pair of BPDs (Discovery DSC-R412) whose two outputs are sampled by a real-time oscilloscope (LeCroy SDA 830Zi-A) and then offline processed in MATLAB. Due to the limited working condition of the electrical amplifier whose operating frequency is from 100 MHz to 4 GHz in our lab [14], we set 10 subcarriers from the zero frequency to null subcarriers to mitigate the ground noise and 40 subcarriers to data subcarriers, making the OFDM signal occupy the frequency from ∼780 MHz to 3.9 GHz. That is, all the experimental parameter settings are the same with the simulation use in subsection 3.1 except for the number of data subcarriers which is set to 40, thus we can only demonstrate the transmission rate up to 25-Gb/s. Note that, both the transmitter and receiver lasers have a claimed linewidth below 10 kHz. Fig. 6(a) plots the experimental results of Q-factor at different fiber launch powers for conventional and polar coded 25-Gb/s CO-OFDM signals over transmission distance up to 320 km. It is shown that system undergoes nonlinear domain when the launch powers are higher than 6 dBm, 5 dBm and 5 dBm for 100 km, 200 km and 320 km transmission respectively. Aided by polar code, performance is significantly improved in both the linear and nonlinear domains, the corresponding code gain in Q-factor of nonlinear domain is shown in Fig. 6(b). Maximum code gains of 6.1 dB, 6 dB and 5.5 dB are obtained in nonlinear region at optimum launch powers of 8 dBm, 6 dBm and 6 dBm for 100 km, 200 km and 320 km transmissions respectively. Also, for a fixed Q-factor, the tolerable launch power offset in nonlinear domain is smaller than that in linear domain owe to the non-Gaussian noise, which is similar to the simulation results.

## 4. Conclusion

In this paper, the performances of high-speed polar coded CO-OFDM system with nonlinear and linear impairments are comprehensively investigated by simulation and experiment for the first time. Results show that for single-channel 320-km 40-Gb/s CO-OFDM system, in nonlinear region,

polar code is slightly affected by nonlinearity-induced non-Gaussian noise but still performs strong robustness. Compared with the conventional approach, with the help of polar code, the optimal fiber launch power is increased by 4 dB, a maximum code gain (in Q-factor) of 3 dB is achieved in dispersion-unmanaged scheme and a 2.9 dB is further enhanced under symmetric dispersion-compensated scheme. In the linear region, polar code gains (in SNR) of 4.5 dB and 6.2 dB are obtained at BER of $2 \times 10^{-3}$ under dispersion-unmanaged and symmetric dispersion-compensated schemes respectively. Meanwhile, polar code significantly resists laser phase noise in both nonlinear and linear domains which effectively relieves the linewidth requirement, achieving a cost-effective system.

## Acknowledgment

The work was supported in part by the National Natural Science Foundation of China under Grant 61501157 and Grant 61433009 and by Natural Science Foundation of Zhejiang Province under Grant LQ16F050004.

## References

[1] I. Roudas, "Coherent optical communication systems," in *WDM Systems and Networks*. New York, NY, USA: Springer, 2012.
[2] S. T. Le *et al.*, "Demonstration of phase-conjugated subcarrier coding for fiber nonlinearity compensation in CO-OFDM transmission," *J. Lightw. Technol.*, vol. 33, no. 11, pp. 2206–2212, Jun. 2015.
[3] W. Shieh, H. Bao, and Y. Tang, "Coherent optical OFDM: theory and design," *Opt. Exp.*, vol. 16, no. 2, pp. 841–859, Jan. 2008.
[4] X. Hong, X. Hong, J. Zhang, and S. He, "Low-complexity linewidth-tolerant time domain sub-symbol optical phase noise suppression in CO-OFDM systems," *Opt. Exp.*, vol. 24, no. 5, pp. 4856–4871, Feb. 2016.
[5] A. Ali, J. Leibrich, and W. Rosenkranz, "Impact of nonlinearities on optical OFDM with direct detection," in *Proc. Eur. Conf. Opt. Commun.*, Sep. 2007, pp. 1–2.
[6] E. Ip and J. M. Kahn, "Compensation of dispersion and nonlinear impairments using digital backpropagation," *J. Lightw. Technol.*, vol. 26, no. 20, pp. 3416–3425, Oct. 2008.
[7] X. Liu, F. Buchali, and R. W. Tkach, "Improving the nonlinear tolerance of polarization-division-multiplexed CO-OFDM in long-haul fiber transmission," *J. Lightw. Technol.*, vol. 27, no. 16, pp. 3632–3640, Aug. 2009.
[8] I. Roudas, N. Kaliteevskiy, P. Sterlingov, and W. A. Wood, "Comparison of analytical models for the nonlinear noise in dispersive coherent optical communications systems" in *Proc. Photon. Conf.*, Sep. 2013, pp. 139–140.
[9] E. Giacoumidis *et al.*, "Fiber nonlinearity-induced penalty reduction in CO-OFDM by ANN-based nonlinear equalization," *Opt. Lett.*, vol. 40, no. 21, pp. 5113–5116, Nov. 2015.
[10] J. Zhang *et al.*, "Comparison of ICI reduction and fiber nonlinearity tolerance for DCS-OFDM and conventional OFDM with equal spectrum efficiency," *IEEE Photon. J.*, vol. 7, no. 1, Feb. 2015, Art. no. 7200206.
[11] M. Bi, S. Xiao, H. He, J. Li, L. Liu, and W. Hu, "Power budget improved symmetric 40-Gb/s long reach stacked WDM-OFDM-PON system based on single tunable optical filter," *IEEE Photon. J.*, vol. 6, no. 2, Apr. 2014, Art. no. 7900708.
[12] F. Chang, K. Onohara, and T. Mizuochi, "Forward error correction for 100 G transport networks," *IEEE Commun. Mag.*, vol. 48, no. 3, pp. S48–S55, Mar. 2010.
[13] A. Bisplinghoff, S. Langenbach, E. S. Vercelli, R. Pastorelli, and T. Kupfer, "Cycle slip tolerant, differential encoding aware, soft-decision FEC," in *Proc. Conf. Opt. Fiber Commun.*, 2015, Paper Tu3B. 2.
[14] L. Liu, S. Xiao, J. Fang, L. Zhang, Y. Zhang, M. Bi, and W. Hu, "High performance and cost effective CO-OFDM system aided by polar code," *Opt. Exp.*, vol. 25, no. 3, pp. 2763–2770, Feb. 2017.
[15] E. Arikan, "Channel polarization: A method for constructing capacity-achieving codes for symmetric binary-input memoryless channels," *IEEE Trans. Inf. Theory.*, vol. 55, no. 7, pp. 3051–3073, Jul. 2009.
[16] E. Arikan, "A performance comparison of polar codes and Reed-Muller codes," *IEEE Commun. Lett.*, vol. 12, no. 6, pp. 447–449, Jun. 2008.
[17] T. Tanimura, Y. Koganei, H. Nakashima, T. Hoshida, and J. C. Rasmussen, "Soft decision forward error correction over nonlinear transmission of 1-Tb/s superchannel," in *Proc. Eur. Conf. Opt. Commun.*, Sep. 2014, Paper Th.1.3.4.
[18] B. P. Smith and F. R. Kschischang, "Future prospects for FEC in fiber-optic communications," *IEEE J. Sel. Topics Quantum Electron.*, vol. 16, no. 5, pp. 1245–1257, Sep. 2010.
[19] I. B. Djordjevic, S. K. Chilappagari, and B. Vasic, "Suppression of intrachannel nonlinear effects using pseudoternary constrained codes," *J. Lightw. Technol.*, vol. 24, no. 2, pp. 769–774, Feb. 2006.
[20] S. L. Jansen, I. Morita, T. C. W. Schenk, N. Takeda, and H. Tanaka, "Coherent optical 25.8-Gb/s OFDM transmission over 4160-km SSMF," *J. Lightw. Technol.*, vol. 26, no. 1, pp. 6–15, Jan. 2008.
[21] X. Liu, S. Chandrasekhar, P. J. Winzer, R. W. Tkach, and A. R. Chraplyvy, "Fiber-nonlinearity-tolerant superchannel transmission via nonlinear noise squeezing and generalized phase-conjugated twin waves," *J. Lightw. Technol.*, vol. 32, no. 4, pp. 766–775, Feb. 2014.
[22] I. Tal and A. Vardy, "How to construct polar codes," *IEEE Trans. Inf. Theory*, vol. 59, no. 10, pp. 6562–6582, Oct. 2013.

[23] X. Yi, B. Xu, J. Zhang, Y. Lin, and K. Qiu, "Theoretical calculation on ICI reduction using digital coherent superposition of optical OFDM subcarrier pairs in the presence of laser phase noise," *Opt. Exp.*, vol. 22, no. 25, pp. 31192–31199, Dec. 2014.
[24] L. Liu, S. Xiao, M. Bi, and L. Zhang, "Comparison study of long-haul 100-Gb/s DDO-OFDM and CO-OFDM WDM systems," *J. Opt. Soc. Korea*, vol. 20, no. 5, pp. 557–562, Oct. 2016.
[25] Y. Tian, M. Bi, H. He, J. Li, and W. Hu, "Power budget improvements using grouped pilot channel estimation for OFDM-PON," in *Proc. Conf. Asia Commun. Photon.* Nov. 2013, Paper AF1G. 5.
[26] V. Vgenopoulou, M. S. Erkilinc, R. I. Killey, Y. Jaouen, I. Roudas, and I. Tomkos, "Comparison of multi-channel nonlinear equalization using inverse volterra series versus digital backpropagation in 400 Gb/s coherent superchannel," in *Proc. Eur. Conf. Opt. Commun.*, Sep. 2016, pp. 1–3.